

# The Influence of Solidity on the Performance Characteristics of a Tidal Stream Turbine

Ceri Morris<sup>#1</sup>, Allan Mason-Jones<sup>#</sup>, Daphne O'Doherty<sup>#</sup>, Tim O'Doherty<sup>#</sup>

<sup>#</sup>*School of Engineering, Cardiff University  
Queens Buildings, The Parade, Cardiff, UK*

<sup>1</sup>morrisce3@cf.ac.uk

**Abstract**— The performance characteristics of a tidal stream turbine are critical when assessing its economical viability. The solidity of the rotor, which is a function of the blade chord length and the number of blades, will affect the performance characteristics, from both a power output and a structural loading viewpoint.

This paper investigates the influence of solidity on the performance characteristics of a horizontal axis tidal turbine using experimentally validated CFD models. The solidity was varied by altering the number of blades in the numerical models.

Increasing the solidity was found to increase the peak  $C_{\theta}$  and peak  $C_p$  and reduce the  $\lambda$  at which these occur.  $C_t$  was found to be approximately the same at peak  $C_p$  which was assumed to be the normal operating condition. At  $\lambda$  above peak  $C_p$ , near freewheeling,  $C_t$  continued to increase for the 2 bladed turbine, remained approximately constant for the 3 bladed turbine and decreased for the 4 bladed turbine, indicating that higher solidity rotors would have to withstand lower loads in the event of a failure. In addition, the thrust per blade was shown to increase with a reduction in the number of blades.

**Keywords**— Solidity, Performance, Tidal Stream Turbine

## I. INTRODUCTION

It is widely understood and accepted that in order to ensure security of supply, the energy mix must diversify to include a wider variety of resources [1]. There is also a drive to reduce the emissions that contribute to global warming in an attempt to mitigate the effects of climate change. The current targets for the EU are set at a 20% reduction from the 1990 baseline level by 2020, with 20% of total energy consumption derived from renewable sources [2].

Renewables such as wind and solar photovoltaic (PV), whilst providing a valuable contribution to the energy mix, are unpredictable in the medium to long term and therefore cannot replace conventional fossil fuelled power plants. The energy in the tides can be accurately predicted weeks, months and even years in advance. This predictability is the main advantage of tidal energy. Another advantage is the limited visual impact when compared with, for example, wind turbines.

Tidal energy technologies generally fall into two categories; tidal range and tidal stream. Tidal range schemes extract energy by using a barrage or impoundment to create a head difference and then releasing water through turbines to generate electricity whereas tidal stream devices extract

energy directly from the currents. This paper is based on tidal stream devices and investigates the effect of solidity on performance characteristics. The performance of a tidal stream device is crucial in determining its financial viability and length of payback and will be affected by factors including blade or hydrofoil design and solidity. Any changes in performance with blade deflection under loading will also affect the overall efficiency of a device and its energy extraction over a tidal cycle, again influencing the economics of an installation.

## II. SOLIDITY

The Solidity of a turbine is given by the ratio of the total blade area to the swept area of the rotor and is represented by Equation 1 [3].

$$\sigma = \frac{BC}{\pi R} \quad (1)$$

where B is the number of blades and C is the average chord length.

For a given rotor radius, solidity can therefore be altered by changing the chord length or the number of blades. Although there have been few studies on solidity for horizontal axis tidal turbines (HATTs), findings from work on horizontal axis wind turbines (HAWTs) may be transferable. It has been shown by Hau [4] that increasing the number of blades on the rotor of a HAWT increases its power output but with diminishing returns so that there is a smaller benefit for each additional blade. It was also shown by Hau [4] that an increase in the number of blades reduces the operational range and the optimum tip speed ratio ( $\lambda$ ). The increased power and reduction in both operational range and optimum  $\lambda$  was shown by [5] to also be true for a vertical axis tidal turbine (VATT) but only two blade configurations were modelled and therefore the diminishing returns could not be confirmed. Shiono et al. [6] found that for a fixed number of blades the power output of a VATT increased with solidity from a solidity of 0.108 to 0.179 and then decreased with further increases in solidity.

The majority of horizontal axis wind turbines (HAWTs) are 3 bladed and the reasons for this include aesthetics, noise and engineering considerations. It is generally thought that 3 bladed rotors are more aesthetically pleasing than 2 bladed rotors and are quieter due to a lower rotational speed [7]. Although aesthetics will not be an issue for tidal stream

turbines, noise generation may be a problem for marine life [8]. In addition to noise, higher rotational speeds may also increase the risk of cavitation [9] and injury or death to marine mammals.

The number of blades is a particular concern for pile driven and gravity based structures since as a blade passes in front of the support stanchion, or behind for some designs, tower shadow effects occur, leading to a reduction in torque and thrust [10]. The more blades a rotor has, the smaller the relative effect of one blade passing the stanchion will be and the smaller the fluctuations in torque and thrust.

The solidity values used for the work presented in this paper and the associated number of blades are shown in TABLE I

Turbine Solidity  $V$ , where solidity was varied by changing the number of blades whilst keeping the blade design constant.

TABLE I  
TURBINE SOLIDITY VALUES

No of Blades,	Solidity, $\sigma$
2	0.14
3	0.21
4	0.28

### III. PERFORMANCE CHARACTERISTICS

The turbine performance characteristics, that is the power, torque and axial thrust, have all been non-dimensionalised using Froude's Momentum Theory for an actuator disk, described by Myers and Bahaj [11], [12]. Experimental validation of a scaled turbine is described by Tedds et al [13] with non-dimensional scaling to a 10m diameter turbine described by Mason-Jones et al [14]. The performance characteristics considered for this study are therefore presented in these non-dimensional forms, that is the power coefficient ( $C_p$ ), the torque coefficient ( $C_\theta$ ) and the thrust coefficient ( $C_T$ ).

$C_p$  is the ratio of the power extracted by the turbine to the available power from the tidal flow.  $C_\theta$  is given by the ratio between the torque generated via the hydrodynamic lift and the maximum theoretical torque.  $C_T$  is given by the ratio between the axial thrust along the rotational axis of the turbine, generated via the hydrodynamic drag on the rotor blades and hub, and the axial thrust over the swept area of the turbine. This paper considers the variation in these coefficients with  $\lambda$ , for the 2, 3 and 4 bladed turbines, and then compares the results for each configuration.

### IV. CFD MODELLING

The operational performance characteristics of a 3 bladed HATT which utilised a Wortmann FX 63-137 profile, with a  $33^\circ$  twist from the blade root to tip have previously been extensively studied [13], [14], [15]. The work discussed in this paper is derived from the modelling of 10 m diameter TSTs with 2, 3 and 4 blades, (Figure 1) each with the same blade profile and twist and an average chord length of 1 m. The blade tip pitch angles were  $3^\circ$ ,  $6^\circ$  and  $9^\circ$  for the 2, 3 and 4 bladed rotors respectively.

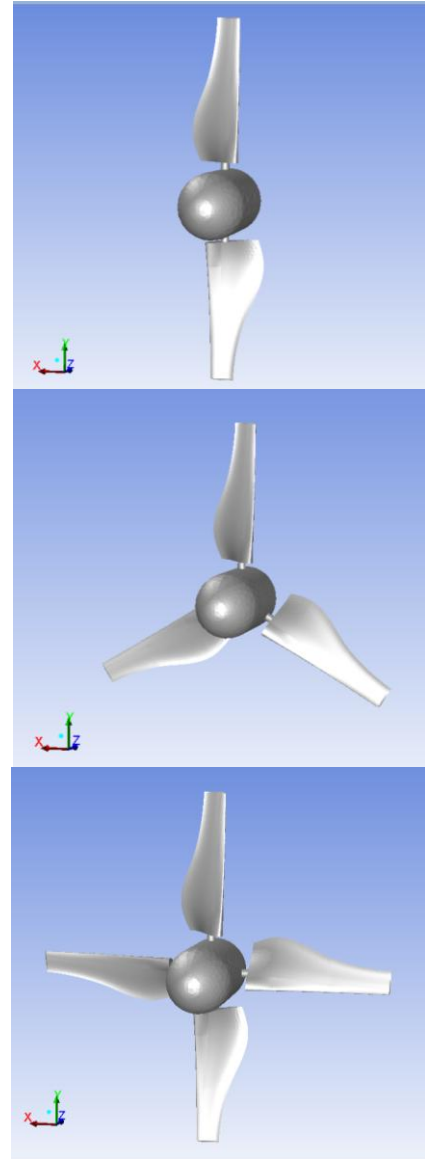


Figure 1: Turbine configurations

In summary, the CFD domain was defined as a rectangular (sea) domain with a width and depth of  $5D$  and a length of  $40D$  to ensure the turbine was fully isolated from any boundary effects. The turbine was located  $10D$  downstream from the inlet boundary such that its rotational axis was set at  $35\text{ m}$  below the water. An axially aligned cylindrical domain (turbine) was subtracted from the rectangular domain to form a Multiple Reference Frame (MRF) with a non-conformal

interface between the sea and turbine volumes. The MRF was centred about the rotational axis of the turbine and extended 0.5 m upstream and 1.5 m downstream. The domain can be seen in Figure 2.

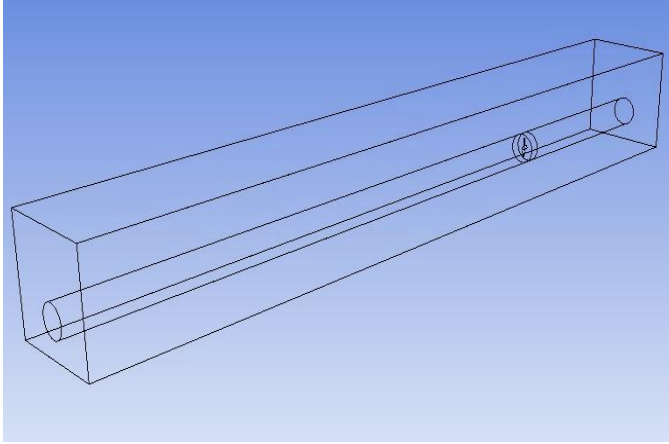


Figure 2: CFD Domain

A quad meshing scheme was applied to the sea channel which incorporated  $\sim 0.5M$  cells. Given the complex shape of the blades and geometry between the blades and the hub, the MRF volume was meshed with a tetrahedral hybrid scheme, with a blade surface mesh as shown in Figure 3. The number of cells within the MRF was  $\sim 0.9M$  for the 2 bladed turbine models,  $\sim 1.4M$  for the 3 bladed turbine models and  $1.8M$  for the 4 bladed turbine models, which provided a suitable cell size for grid independence for the characteristics discussed in this paper.

The outer boundaries of the domain were modelled as stationary walls with zero-shear applied. In order to maintain an economical computational model, free surface interaction between the water and air was not included.

For all the CFD models a water density of  $1025 \text{ kg/m}^3$  and a dynamic viscosity of  $0.00111 \text{ kg/ms}$  were used. At 1 turbine diameter upstream of the rotational plane of the turbine the turbulence intensity was around 10%, which has been shown to be realistic for a tidal stream site [16], [17]. To model the upstream flow regime a plug flow velocity of  $3.1 \text{ m/s}$  was applied at the inlet. The viscous model used was the Reynolds Stress Model (RSM), which includes anisotropy of the turbulent eddy viscosity, and has been shown to be suitable to modelling the performance of a HATT [14].

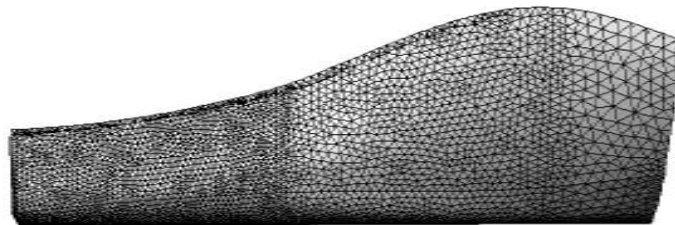


Figure 3: Mesh on blade surface

## V. RESULTS & DISCUSSION

### A. Torque

Figure 4 shows that the cut-in  $C_0$  of the 2 bladed turbine is 0.025. The  $C_0$  then increases, reaching a peak of 0.114 at a  $\lambda$  of 2.43. The increase is approximately linear from a  $\lambda$  of 1 until peak  $C_0$  (at a rate of 0.052). After the peak,  $C_0$  decreases, again linearly but at a slower rate (0.020), until it reaches 0 at the freewheeling  $\lambda$  of around 8.1. This is the maximum velocity at which the turbine would rotate due to the hydrodynamic forces imparted on the blades by the tidal current. For the turbine to rotate at a  $\lambda$  greater than this, it would have to be driven by a motor and would be acting as a pump.

The  $C_0$  curves for the 3 and 4 bladed turbines are also shown in Figure 4. They follow the same general trend as those of the 2 bladed turbine, with an almost linear increase from  $\lambda = 1$  to peak  $C_0$  and a linear but slower decrease from peak  $C_0$  to freewheeling.

For the 3 bladed turbine, the model predicts a cut-in  $C_0$  of 0.05, and a peak  $C_0$  of 0.158, both higher than those of the 2 bladed turbine. The curve can be seen to increase from  $\lambda = 1$  with a rate of 0.105 to the peak which occurs at a  $\lambda$  of 1.94. Freewheeling  $\lambda$  occurs at around 7.1, lower than the 2 bladed turbine, with the rate of decrease being 0.031.

For the 4 bladed turbine, the prediction of cut-in  $C_0$  has again increased, to 0.07, and the peak  $C_0$  has increased to 0.188. The  $\lambda$  at which peak  $C_0$  occurs has further decreased, to around 1.8, and the freewheeling  $\lambda$  has reduced to 6.4. The linear increase from  $\lambda = 1$  to the peak has a rate of 0.125 and the rate of decrease from the peak is 0.042.

It is clear from Figure 4 that the cut-in  $C_0$  increases with the number of blades. This is due to the resultant force on each blade being multiplied by the number of blades. The rate of increase of cut-in  $C_0$  also increases with the number of blades with a larger difference between 3 and 4 blades than between 2 and 3 blades. Near  $\lambda = 0$ , there is little to no flow over the rear surface of the blade (upper portion of the hydrofoil) and hence there is very little lift and the torque is dominated by the reaction force as the fluid is deflected around the blade. The increase in pitch angle with the number of blades means that the resultant force per blade also increases.

The increase in peak  $C_0$  with the number of blades is in agreement with the findings for a Vertical Axis Wind Turbine by Roh and Kang [18], who found that peak  $C_0$  increased with solidity for  $\sigma$  between 0.033 and 0.08. One consequence of this is that the 4 bladed turbine would require the largest diameter of drive shaft and the 2 bladed turbine the smallest, implying that the cost of the drive shaft could increase with the number of blades. Based on these results, maintaining a

constant shear stress would require a ~25% increase in the shaft diameter from the 2 bladed turbine to the 4 bladed turbine. This is based on a simplistic consideration that  $\tau = 16T/\pi D^3$ .

It is also clear from Figure 4 that the  $\lambda$  at which both peak  $C_0$  and freewheeling occur decrease with an increase in the number of blades. This is because the optimum pitch angle increases with the number of blades and hence a lower value of  $\lambda$  is required to achieve the optimum lift to drag ratio. If a traditional mechanical power train were used, this may result in additional stages within the gearbox for a higher number of blades, with the increased costs and losses associated. All of the turbines have a torque curve typical of a HATT, [19], [14].

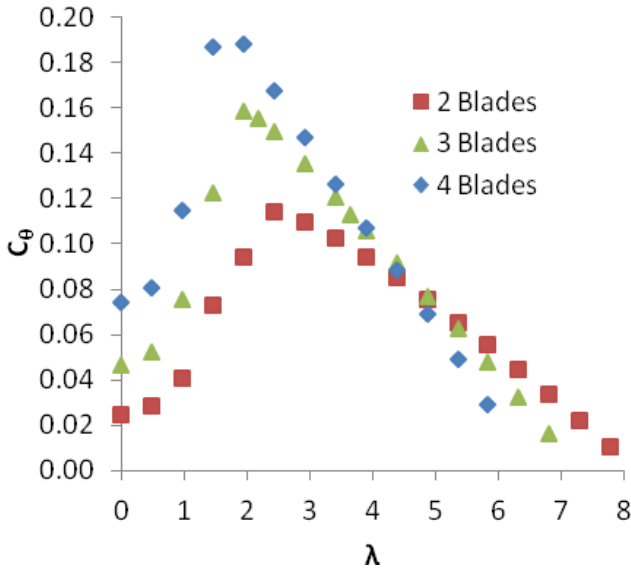


Figure 4  $C_0$  vs  $\lambda$  for the 2,3 and 4 bladed turbines

Figure 5 shows the  $C_0$  curves for all three turbine configurations, normalised with respect to maximum  $C_0$  and maximum  $\lambda$  for each turbine. Aside from at start up and at very low values of  $\lambda$ , the curves of the 3 and 4 bladed turbines show very good correlation. The 2 bladed turbine data do not compare as well but still fall within 10% of the values for the other turbine configurations at  $\lambda$  from peak  $C_0/C_0 \text{ max}$  to freewheeling. Therefore, for this blade design, with knowledge of the torque characteristics of one turbine configuration, a reasonable estimation of the torque characteristics of another configuration over the majority of its operational range could be made. In practical terms, once the freewheeling  $\lambda$  had been established, the  $\lambda$  at which peak  $C_0$  occurs could be estimated to within ~7% and vice versa.

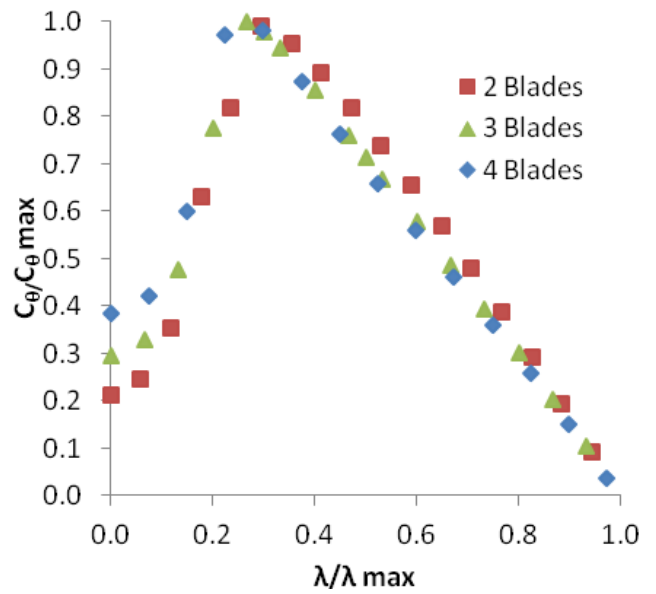


Figure 5 Normalised  $C_0$  vs normalised  $\lambda$  for the 2, 3 and 4 bladed turbines

### B. Power

Figure 6 shows the power curve for the 2, 3 and 4 bladed turbines. Peak  $C_p$  for the 2 bladed turbine was found to be 0.37, occurring at a  $\lambda$  of 4.4. Again, freewheeling occurs around 8.1. The  $C_p$  curves of the 3 and 4 bladed turbines also follow the same general trend as those of the 2 bladed turbine. Peak  $C_p$  for the 3 bladed turbine is increased to 0.41 but occurs at a lower  $\lambda$  of around 3.65. Peak  $C_p$  predicted for the 4 bladed turbine is 0.43, which is higher than both the 2 and 3 bladed turbines. It occurs at a  $\lambda$  of around 3.4, lower than both other turbine configurations.

As seen in Figure 6, peak power increases with the number of blades and the tip speed ratio at which peak power occurs decreases. The difference in both peak power and the  $\lambda$  at which it occurs is greater between the 2 and 3 bladed turbines than between the 3 and 4 bladed turbine, with diminishing returns from each additional blade as expected from Hau [4]. In this case the peak  $C_p$  values are 0.37, 0.41 and 0.43, occurring at  $\lambda$  of 4.37, 3.65 and 3.40 for the 2, 3 and 4 bladed turbines respectively.

The operating range is shown to increase with decreasing number of blades, with freewheeling occurring around a  $\lambda$  of 8.1 for the 2 bladed turbine, 7.3 for the 3 bladed turbine and 6.4 for the 4 bladed turbine. This trend has also been shown to occur for HAWTs [4].

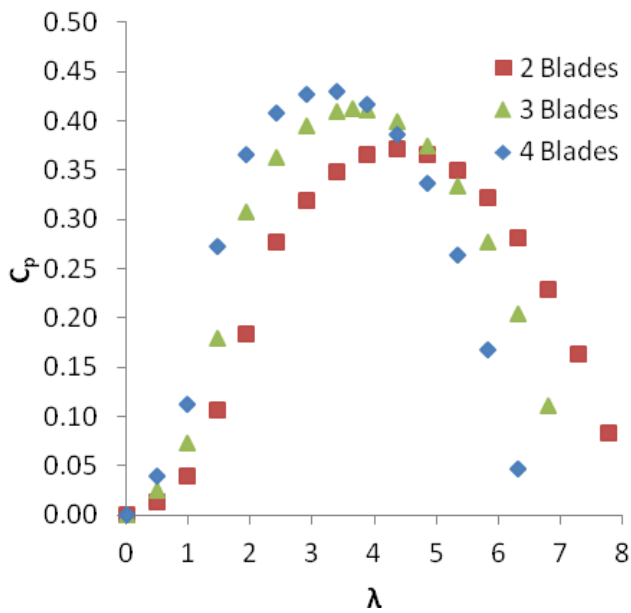


Figure 6  $C_p$  vs  $\lambda$  for the 2, 3 and 4 bladed turbines

Normalising the  $C_p$  curves with respect to maximum  $\lambda$  and maximum  $C_p$  for each turbine gives the curves shown in Figure 7. As with the normalised  $C_0$  curves, the data show good correlation for all three turbines, particularly from peak  $C_p$  to freewheeling. The  $\lambda$  at which peak  $C_p$  occurs could be estimated to within  $\sim 6\%$  from the knowledge of the freewheeling  $\lambda$  for any of the configurations. It should be noted that the asymmetry of the correlation is simply due to  $\lambda$  being normalised against  $\lambda_{max}$ , whereas if the normalisation was based on  $\lambda$  at peak  $C_p$  the correlation would be symmetrical.

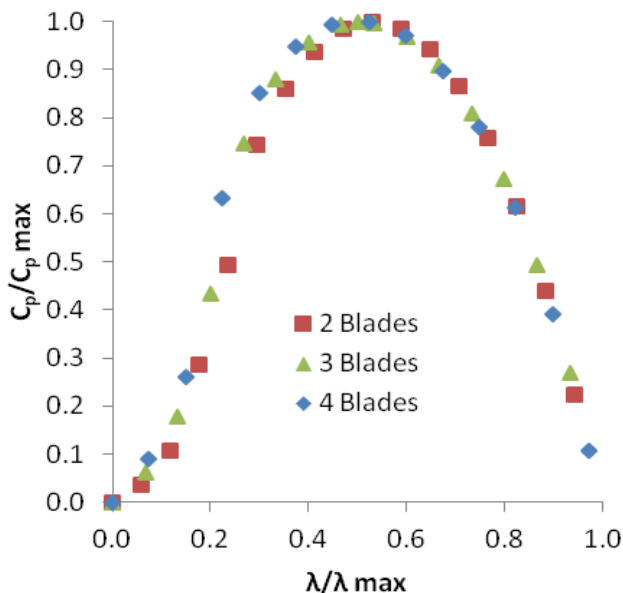


Figure 7 Normalised  $C_p$  vs normalised  $\lambda$  for the 2, 3 and 4 bladed turbines

### C. Thrust

The  $C_t$  of the 2 bladed turbine when stationary ( $\lambda=0$ ) is 0.17, as shown in Figure 8. This then increases with  $\lambda$ , reaching a maximum of 1.06 at freewheeling. Since operating at peak power would result in the greatest quantity of electricity being produced, it is assumed that this would be the normal operating condition. If the 2 bladed turbine was operated at peak power, i.e. a  $\lambda$  of 4.4, the  $C_t$  would be 0.82.

As expected the  $C_t$  of the 3 bladed turbine is higher when stationary than the  $C_t$  of a stationary 2 bladed turbine due to the higher solidity, with a predicted  $C_t$  of 0.25. The prediction of  $C_t$  for the 4 bladed turbine is higher again, at 0.34, due to its even higher solidity.

For the 3 bladed turbine the  $C_t$  predicted at the  $\lambda$  corresponding to maximum  $C_p$  is 0.85 which is slightly higher than under the same condition for the 2 bladed turbine. Unlike with the 2 bladed turbine, the  $C_t$  of the 3 bladed turbine does not continue to increase with  $\lambda$  to freewheeling but instead reaches a maximum at a  $\lambda$  of 5.8, before decreasing slightly to freewheeling. Peak  $C_t$  is lower at 0.94, compared with 1.06 for the 2 bladed turbine.

As with the 3 bladed turbine, the  $C_t$  for the 4 bladed does not continue to increase with  $\lambda$  to freewheeling. It reaches a maximum of 0.86, the lowest of the three configurations, at a  $\lambda$  of 3.9 before falling to 0.77 at freewheeling. The  $C_t$  of the 4 bladed turbine at peak power is 0.85, which is the same as that of the 3 bladed turbine at peak power.

Figure 8 shows that at lower  $\lambda$  the  $C_t$  of the 4 bladed turbine is highest and the  $C_t$  of the 2 bladed turbine is lowest but that at higher  $\lambda$  this is reversed. It also shows that at the freewheeling  $\lambda$  for each turbine the  $C_t$  of the 2 bladed turbine is still increasing, the  $C_t$  of the 3 bladed turbine is steady and the  $C_t$  of the 4 bladed turbine is decreasing. This is because the pitch angle increases with the number of blades. Mason-Jones et al. [14] investigated the effect of changing the pitch angle of a 3 bladed turbine, using the same blade design as described in this paper. The findings showed that pitch angle had little effect on  $C_t$  at  $\lambda$  less than 1.2 but with a pitch angle less than  $6^\circ$ ,  $C_t$  continues to increase with  $\lambda$  to freewheeling whereas with a pitch angle above  $6^\circ$ ,  $C_t$  reaches a maximum before decreasing toward freewheeling.

The consequences of this behaviour at high  $\lambda$  would be important when designing the turbine to withstand loads in the event of a failure of the control or braking system with the steady load on the 3 bladed turbine and the decreasing load on the 4 bladed turbine being an advantage. The peak  $C_t$  for each turbine over the operating range are 1.06, 0.94 and 0.86 for the 2, 3 and 4 bladed turbines respectively. It is therefore clear that the peak  $C_t$  is highest for the 2 bladed turbine and lowest for the 4 bladed turbine. This means that if these blades were used for a fixed pitch 2 bladed rotor, the control system would need to be very reliable or the blade roots strong enough to withstand the high bending moments that would result from

the high thrust in the event of a failure. The alternatives would be to have:

- 1) variable pitch blades, which could increase the cost and complexity of the device and potentially reduce reliability.
- 2) bend-twist coupled blades where the tip pitch angle would increase with deflection.

In order to assess the  $C_t$  for each turbine under normal operating conditions it is necessary to compare the  $C_t$  of each turbine at the  $\lambda$  at which it is run. If each turbine is run at peak power the  $C_t$  values for the 2, 3 and 4 bladed turbines are 0.82, 0.85 and 0.85 respectively. Hence it can be seen that under normal conditions the  $C_t$  of each turbine is 0.84 ( $\pm 2\%$ ).

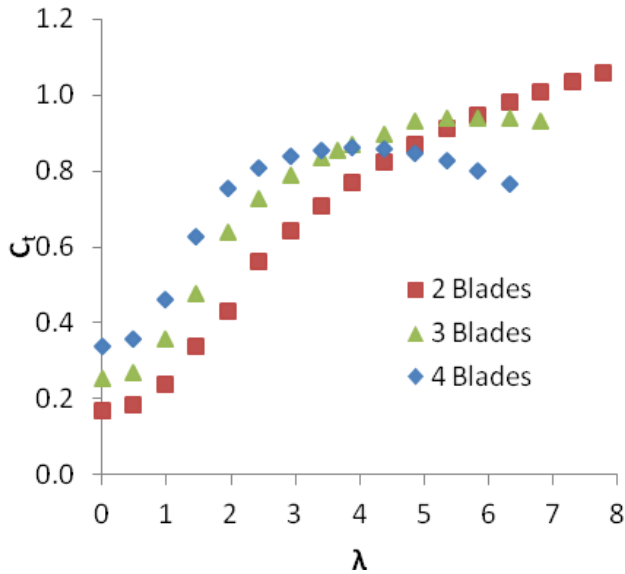


Figure 8  $C_t$  vs  $\lambda$  for the 2, 3 and 4 bladed turbines

When comparing the normalised  $C_t$  curves for each turbine, shown in Figure 9, it is clear that unlike the  $C_p$  and  $C_0$  characteristics none of the curves overlay and that the  $C_t$  curve of one configuration cannot be estimated from the  $C_t$  curve of another.

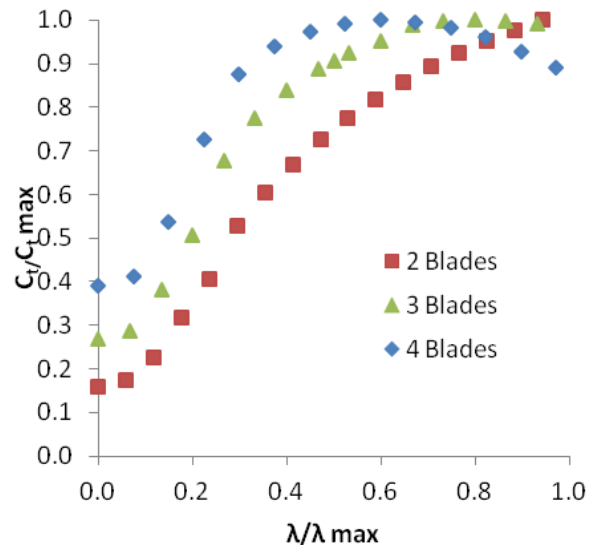


Figure 9 Normalised  $C_t$  vs normalised  $\lambda$  for the 2, 3 and 4 bladed turbines

Although the thrust load on each turbine is of a similar magnitude under normal operating conditions, when the number of blades is considered, the thrust per blade is as shown in Figure 10. It is clear that at  $\lambda$  below 2, the thrust per blade is very similar for all three turbine configurations. At  $\lambda$  above 2, the curves diverge with the thrust per blade on the 2 bladed turbine highest and the thrust per blade on the 4 bladed turbine lowest. The thrust per blade on the 4 bladed turbine peaks at 79.2 kN at a  $\lambda$  of 3.9 before falling to 70.5 kN at the freewheeling  $\lambda$ . Peak thrust per blade on the 3 bladed turbine is 116.0 kN at a  $\lambda$  of 6.3 and this remains fairly steady to freewheeling with only a slight decrease to 115.0 kN. The thrust per blade on the 2 bladed turbine keeps increasing to freewheeling at which it reaches 200.3 kN. Comparing the thrust per blade with that of the 4 bladed turbine, there is an increase of a factor of approximately 1.5 for the 3 bladed turbine and 2.5 for the 2 bladed turbine. Under normal operating conditions, which are assumed to be at peak power, the thrust per blade is 151.0 kN, 104.6 kN and 78.5 kN for the 2, 3 and 4 turbines respectively. Therefore, even under these conditions, the thrust per blade is 1.3 times greater for the 3 bladed turbine and 1.9 times greater for the 2 bladed turbine when comparing with the thrust per blade on the 4 bladed turbine. This blade design is therefore better suited to a 3 or 4 bladed rotor since, even at peak power the load on each blade of a 2 bladed rotor is much greater and, in the case of a failure, continues to increase to freewheeling.

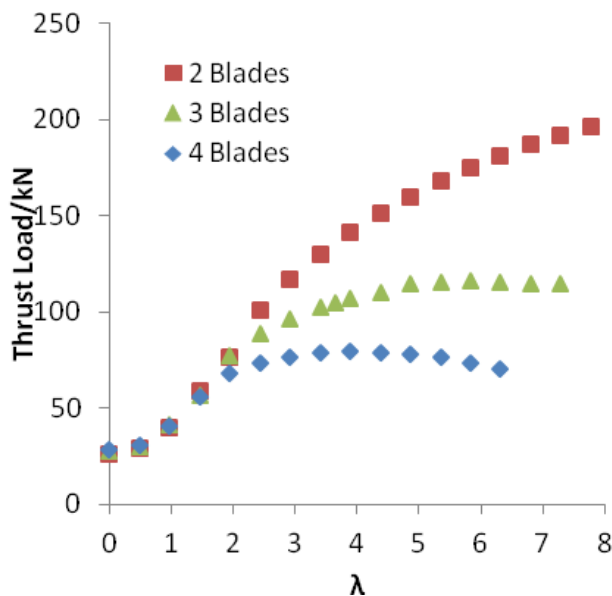


Figure 10 Thrust per blade vs  $\lambda$  for the 2, 3 and 4 bladed turbines

## VI. CONCLUSIONS

This paper has shown that there is an increase in torque, and hence power, with an increasing number of blades, in agreement with previous studies on wind turbines and vertical axis tidal turbines [4], [18]. There is an associated reduction in the  $\lambda$  at which peak power occurs.

For the given blade design it has also been shown that although under normal operating conditions,  $C_t$  is slightly higher for 3 and 4 bladed turbines, the thrust per blade is much higher for 2 bladed turbine. Therefore, although the loads which the stanchion, drive train etc. must withstand would be of a similar magnitude regardless of the number of blades, the blades themselves would need to be designed for much greater loads with fewer blades. However, more blades would mean an increased cost of manufacture, increased cost and complexity of installation and maintenance.

## ACKNOWLEDGMENT

The authors wish to acknowledge the financial support of LCRI, EPSRC and HPC Wales.

## REFERENCES

- [1] DECC, 2013. *UK Renewable Energy Roadmap Update 2013*. London: Crown copyright, Department of Energy & Climate Change
- [2] European Union Committee, 2008. *27th Report of Session 2007–08 - The EU's Target for Renewable Energy: 20% by 2020*. London : The Stationery Office Limited
- [3] Duquette, M. and Visser, K.D., 2003- Numerical implications of solidity and blade number on rotor performance of horizontal-axis wind turbines. *Journal of Solar Energy Engineering* 125(4), pp. 425-432.
- [4] Hau, E., 2006. *Wind Turbines: Fundamentals, technologies, application, economics*. 2<sup>nd</sup> edition.

- [5] Consul, C.A., Willden, R.H.J., Ferrer, E., McCulloch, M.D. Influence of Solidity on the Performance of a Cross-Flow Turbine. *8th European Wave and Tidal Energy Conference*, Uppsala, 7-10 September 2009.
- [6] Shiono, M., Suzuki, K., Kiho, S., 2000. An Experimental Study of the Characteristics of a Darrieus Turbine for Tidal Power Generation. *Electrical Engineering in Japan* 132(3), pp. 38-47.
- [7] Cottrell, J., 2002. The mechanical design, analysis and testing of a two-bladed wind turbine hub. National Renewable Energy Laboratory. Technical Report. NREL/TP-500-26645. [Online] Available at: <http://www.nrel.gov/docs/fy02osti/26645.pdf> [Accessed 6 April 2013]
- [8] DTI, 2007. *Economic viability of a simple tidal stream energy capture device*. London: Department of Trade and Industry.
- [9] Wadia, M., Meunier, M., Olsen, D., McEwen, L., 2011. Composite Blades for Tidal Turbines Versus Wind Turbines at Multi-Megawatt Scale. *9th European Wave and Tidal Energy Conference*. Southampton, 5-9 September 2011.
- [10] Mason-Jones, A., O'Doherty, D.M., Morris, C.E., O'Doherty, T., 2013. Influence of a velocity profile & support structure on tidal stream turbine performance. *Renewable Energy* 52, pp. 23-30.
- [11] Myers LE and Bahaj AS, 2009, Experimental analysis of the flow field around horizontal axis tidal turbines by use of scale mesh disk rotor simulators, *Ocean Engineering*, Vol 37, pp 218-227
- [12] Myers LE and Bahaj AS, Near wake properties of horizontal axis marine current turbines, *8th European Wave and Tidal Energy Conference*, 2009, Uppsala, Sweden
- [13] Tedds, S.C., Poole, R.J., Owen, I., Najafian, G., Bode, S.P., Mason-Jones, A., Morris, C., O'Doherty, T., O'Doherty, D.M. Experimental Investigation of Horizontal Axis Tidal Stream Turbines. *9th European Wave and Tidal Energy Conference*. Southampton, 5-9 September 2011.
- [14] Mason-Jones A, O'Doherty DM, Morris CE, O'Doherty T, Byrne CB, Owen I, Tedds SC and Poole RJ. Non-dimensional Scaling of tidal stream turbines. *Energy*:
- [15] Mason-Jones A, 2010, Performance assessment of a horizontal axis tidal turbine in a high velocity shear environment, PhD, Cardiff University
- [16] McCann, G. Thomson, M., Hitchcock, S. Implications of Site-Specific Conditions on the Prediction of Loading and Power Performance of a Tidal Stream Device. *2nd International Conference on Ocean Energy*, Brest, 15-17 October 2008.
- [17] Osalusi, E., Side, J., Harris, R., 2009. Structure of turbulent flow in EMEC's tidal energy test site. *International Communications in Heat and Mass Transfer* 36(5), pp. 422-431.
- [18] Roh, S.C., and Kang, S.H., 2013. Effects of a blade profile, the Reynolds number, and the solidity on the performance of a straight bladed vertical axis wind turbine. *Journal of Mechanical Science and Technology* 27 (11), pp. 3299-3307.
- [19] Orme, J.A.C. and Masters, I. Design and testing of a direct drive tidal stream generator. *3rd International Conference on Marine Renewable Energy*. Blyth, 6-9 July 2004.